Journal of Natural Gas Science and Engineering 34 (2016) 449–457

Contents lists available at ScienceDirect

Journal of Natural Gas Science and Engineering

journal homepage: www.elsevier.com/locate/jngse

Effect of fracturing fluid immersion on methane adsorption/desorption of coal

Xiangchen Li*, Yili Kang

State Key Laboratory of Oil and Gas Reservoir Geology and Exploitation, Southwest Petroleum University, Chengdu, Si chuan, 610500, China

ARTICLE INFO

Article history:
Received 28 March 2016
Received in revised form
5 July 2016
Accepted 6 July 2016
Available online 9 July 2016

Keywords:
Coalbed methane
Fracturing fluid
Adsorption
Desorption
Pore structure
Surface functional groups

ABSTRACT

Fracturing fluid intrusion into coal seam may cause serious change in the methane adsorption/desorption behaviors. Isothermal adsorption experiments of raw coal and immersed coal samples were carried out to investigate the adsorption/desorption behaviors of methane. The surface free energies of the samples were calculated from the isothermal adsorption results. The functional groups at surface of the samples were monitored by Fourier transform infrared spectroscopy. The pore structure of the coal samples was observed by scanning electron microscopy. Solid-liquid surface interactions were determined by using wetting contact angle and spontaneous imbibition methods. The results showed that the methane adsorption capacity in samples immersed with the fracturing fluids had reduced when compared with the raw coal and formation water immersion treated sample. Due to the reduction of the characteristic pressures after the fracturing fluid immersion, a greater pressure drop was required to enter the effective desorption stage. The changes of the surface free energies during desorption were greater than that of adsorption, which showed that coal had a stronger adsorption affinity to methane during desorption. The surface properties and pore structure of the coal samples had changed after the fracturing fluid immersion, which led to an obvious difference of adsorption/desorption behaviors between the samples. Properties and factors affecting methane adsorption/desorption on immersed coal were useful to understand the methane transport in coal formation after hydraulic stimulation.

1. Introduction

Coalbed methane (CBM) is a high-quality natural-gas resource present in large quantity. The exploitation of CBM is firstly conducted by desorption followed by diffusion and finally seepage (McKee et al., 1989; Mazzotti et al., 2009). The key point at improving CBM recovery is to reasonably allocate the methane supply capacity and seepage ability. A coal reservoir shelters complex interactions between gas, liquid, and solid components. Specific interactions between different liquids and coal affect the physical structure and surface properties of CBM, and consequently affect the adsorption/desorption behavior of methane.

Hydraulic fracturing is usually performed to increase methane production in low permeable coal reservoirs. The fracturing fluid penetrates the fracture under positive pressure and imbibes into the matrix pores due to capillary pressure (Chaturvedi et al., 2009; Ghanbari and Dehghanpour, 2015). This technique presents the difficulty to remove the fracturing fluid residue and filtrate after each fracturing operation. Indeed, the residue blocks the fractures and matrix pores. Previous studies have shown that the pore structure had an important effect upon methane transport through the coal matrix (Smith and Williams, 1987; Beamish and Crosdale, 1995). The results from an adsorption experiment demonstrated that the micropore volume was a major parameter in the control of methane adsorption (Clarkson and Bustin, 1999). Coal seam generally contains a certain amount of clay minerals such as kaolinite, montmorillonite, illite, and chlorite among others. The filtrate can act with the clay minerals leading to the expansion of the coal matrix. Even tiny expansions had lead to large changes in permeability due to the small porosity of coal (Puri et al., 1991). Therefore, the main reasons of coal damage are the fracturing plugging and matrix expansion (Olsen et al., 2003).

Moisture inside the coal matrix has significant impact on the methane adsorption capacity and the behavior of methane desorption. Reported studies suggest that the methane adsorption capacity was negatively correlated to the amount of moisture and remained constant at a critical moisture level (Busch et al., 2004;

* Corresponding author.
E-mail address: li_xiangchen@126.com (X. Li).

http://dx.doi.org/10.1016/j.jngse.2016.07.020
1875-5100/

Reeves and Pekot, 2001; Wolf et al., 2003; Day et al., 2008; Gensterblum et al., 2013). A low adsorption capacity and a high Langmuir pressure of coal were observed after fracturing fluid immersion (Chen et al., 2009). A study based uniquely on experimental adsorption isotherms indicated that the CBM recovery depended on desorption rather than adsorption and that the adsorption hysteresis could affect the application of the Langmuir parameters for the understanding of the methane production process (Wang et al., 2014).

Despite the considerable amount of published research, the detailed mechanism of methane adsorption/desorption on CBM after a fracturing fluid immersion remains not fully understood. We therefore studied the methane adsorption/desorption of raw coal and immersed coal on samples treated with a generally used clean fracturing fluid, active water fracturing fluid, or guar gum fracturing fluid. The processes of adsorption and desorption are discussed based on the determination of desorption characteristics and surface free energies of the differently treated samples. The changes in the pore structure and surface properties were analyzed using scanning electron microscopy (SEM), Fourier transform infrared spectroscopy (FTIR), wetting contact angle and spontaneous imbibition methods. The microscopic mechanism of methane adsorption/desorption on immersed coal by fracturing fluid is then discussed.

2. Experimental section

2.1. Coal samples preparation

The coal samples used in this work were collected from the Ningwu Basin in the Northwest of China. The specifications of the coal samples are shown in Table 1. We tested the following fluid systems: formation water, clean fracturing fluid, active water fracturing fluid, and guar gum fracturing fluid. The formula, pH values, and viscosities are summarized in Table 2.

The coal samples were crushed until obtaining a fine powder of 60–80 mesh and dried at 50 °C for 24 h in vacuum. The fracturing fluid was added under stirring to a beaker containing 100 g of the dried and crushed sample. The sample was weighed again after homogenization. The weighed coal sample was transferred into a vessel containing a supersaturated solution of potassium sulfate (K_2SO_4), then weighted continuously until a stable weight was obtained at room temperature. The same procedure was followed for all the different fracturing fluids.

2.2. Isothermal adsorption/desorption measurements

The isotherm parameters were determined using a volumetric method (Siemons et al., 2007; Gruszkiewicz et al., 2009). The samples were submitted to several pressure steps until reaching a maximum pressure of 12 MPa. The procedure for adsorption measurements was as follows: (1) The coal sample was installed in a sample container; (2) The reference container ($V_2 = 85$ ml) and the sample container ($V_3 = 152$ ml) were placed in a water bath and heated until reaching the test temperature; (3) The free volume of the system was determined by introducing helium; (4) After evacuating the container and isolating the sample container from the reference container, methane was introduced into the reference container and allowed to equilibrate; (5) The valve connecting the sample container to the reference container was opened and the system allowed to re-equilibrate after the equilibration of the reference container; (6) Steps 4 to 5 were repeated. The pressure at every testing point was recorded. The isotherm parameters were calculated using standardized conditions of a temperature of 20 °C and a pressure of 1 atm (101.3 kPa). Desorption measurements were performed as the reversible process of the adsorption measurements. (see Fig. 1)

2.3. Characterization of the pore structure and surface properties

The characteristics of the pore structure were observed using a scanning electron microscope (Quanta 450, FEI). Small specimens were selected from the blown-off surfaces of the raw coal and fracturing fluid immersed coal samples. The coal surfaces were coated with a thin layer of gold after cleaning with alcohol to enhance the conductivity. A relatively flat surface was chosen as the observation plane.

The functional groups at the surface of the coal samples were investigated by Fourier transform infrared spectroscopy (WQF-520 FTIR). The wetting contact angles were measured using the optical contact angle measurement instrument (DSA100, Kruss). The imbibition experiments with the formation water and fracturing fluids were conducted using a home-built imbibition equipment (Li et al., 2014).

2.4. Data analysis

2.4.1. Adsorption volume calculation

The volume of the coal sample was determined as follows:

$$V_s = \frac{(P_2 \times V_2)/(Z_2 \times T_2) + (P_3 \times V_3)/(Z_3 \times T_3) - (P_1 \times V_1)/(Z_1 \times T_1)}{P_2/(Z_2 \times T_2) - P_1/(Z_1 \times T_1)} \quad (1)$$

where V_s was the volume of the coal sample in cm^3; P_1, P_2, and P_3 were the equilibrium pressure, initial pressure of the reference container, and the initial pressure of the sample container in MPa, respectively; T_1, T_2 and T_3 were the equilibrium temperature, the initial temperature of the reference container, and the initial temperature of the sample container in K, respectively; V_1, V_2, and V_3 were the system volume, the volume of the reference container, and the volume of the sample container in cm^3, respectively; Z_1, Z_2, and Z_3 were the compressibility factor of the gas under equilibrium condition, the compressibility factor of the initial gas in the reference container, and the compressibility factor of the initial gas in the sample container, respectively.

The free space volume of the sample container was determined as follows:

$$V_f = V_0 - V_s \quad (2)$$

where V_f was the free space volume in cm^3; V_0 was the volume of the sample container in cm^3; and V_s was the volume of the coal sample in cm^3.

On the basis of the equilibrium pressure and temperature of the reference container and of the sample container, the adsorption

Table 1
Coal petrography and proximate analysis of the coal samples.

Vitrinite reflectance (%)	Vitrinite (%)	Liptinite (%)	Inertinite (%)	Mineral (%)	Moisture (%)	Ash yield (%)	Volatile (%)	Fixed-carbon content (%)
1.02	59.9	1.5	37.1	1.5	1.28	8.88	34.32	55.52

Table 2
Fracturing fluid composition and physical characteristics.

Fracturing fluid	Formula	pH	Viscosity (mPa s)
Active water	1%KCl + 0.3% cleanup additive(CF-5E) + 0.1% bactericide(CJSJ)	7	1
Guar gum	0.3% guar gum + 0.2% cleanup additive(CF-5E) + 0.5% anti-swelling agent(COP) + 0.1% bactericide(CJSJ) + 0.03% gel breaker(TJZP)	8	3
Clean	1% surfactant(FYBS) + 0.5% organic salt(FYGB) + 0.02%breaker (OP-10)	7	1.8

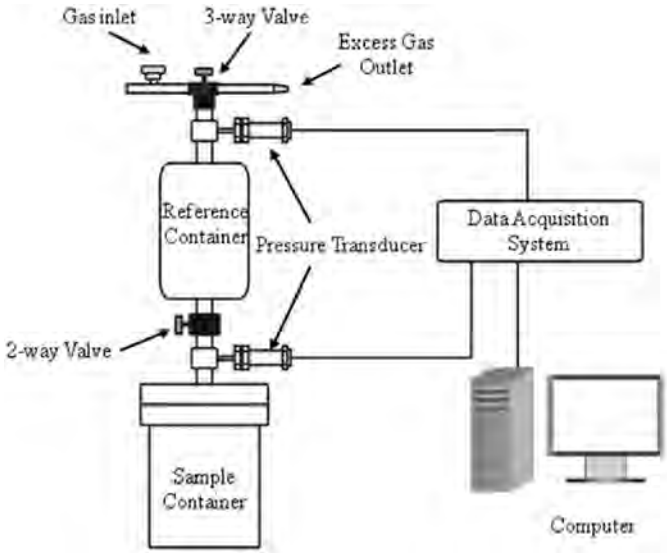

Fig. 1. Diagram of the t experimental setup for methane adsorption/desorption measurements.

volume at different equilibrium pressure was determined as follows:

$$PV = nZRT \tag{3}$$

where P was the gas pressure in MPa; V was the gas volume in cm^3; n was the number of moles of gas in mol; Z was the compressibility factor in MPa; R was the molar gas constant in J mol^{-1} K^{-1}; and T was the equilibrium temperature in K.

The number of moles of gas in the sample container before and after equilibrium was calculated for each pressure as follows:

$$n_i = n_1 - n_2 \tag{4}$$

where n_i was the number of moles of gas in mol; n_1 was the number of moles of gas in the sample container before equilibrium in mol; and n_2 was the number of moles of gas in the sample container after equilibrium in mol.

Hence, the adsorption volume under each pressure was as follows:

$$V_{ads} = V_i/G_C = (n_i \times 22.4 \times 1000)/G_C \tag{5}$$

where V_{ads} was the adsorption volume in $cm^3 \cdot g$; V_i was the total volume of adsorption methane in cm^3; G_C is the mass of the coal sample in g.

2.4.2. Langmuir model

The Langmuir isotherm model is widely used to describe the methane isothermal adsorption on coal fitting the experimental data (Busch and Gensterblum, 2011). Because of the heterogeneous organic matter of the coal, one or more assumptions of the theory are violated. Hence, the application of the Langmuir equation was considered empirical and was as follows:

$$V = \frac{V_L P}{P_L + P} \tag{6}$$

where V represented the adsorption quantity of the coal sample at a methane pressure P in cm^3/g; V_L was the maximum adsorption quantity of the coal sample under a dry condition in cm^3/g; P_L was the Langmuir pressure constant that represents the methane pressure at the half maximum of the total adsorbed quantity in MPa.

2.4.3. Freundlich model

The Freundlich equation is one of the earliest empirical equations used to describe equilibrium and is as follows:

$$V = kP^{1/n} \tag{7}$$

where V is the methane adsorption capacity for one gram of coal in cm^3/g; P is the equilibrium pressure in MPa; k and n are the constants that depend on the adsorbent, adsorbate, and temperature; n represents the strength of adsorption. The trend of the adsorption isotherm becomes more nonlinear when the value n is increasing.

2.4.4. Characteristic pressure of desorption

Desorption is the reverse process of adsorption and determines the recovery efficiency of a coalbed methane reservoir. The desorption of immersed coal was investigated by analyzing the characteristic pressures. The desorption efficiency was defined as the desorbed amount of methane for one drop of a unit pressure (Meng et al., 2014). The coalbed methane desorption efficiency could be characterized as the first derivative of the Langmuir equation:

$$\eta = V' = \frac{V_L P_L}{(P + P_L)^2} = \left(\frac{\alpha}{\beta}\right)^2 \tag{8}$$

With $\alpha = \sqrt{V_L P_L}$, $\beta = P + P_L$.

The curvature of the Langmuir equation was quantitatively characterized as follows:

$$K_L = \frac{2\alpha^2 \Big/ \beta^3}{\left(1 + \alpha^4 \Big/ \beta^4\right)^{3/2}} \tag{9}$$

Equations which depended on the pressure, transition pressure, and the threshold pressure were characterized by the first derivative of the curvature (Table 3). The desorption efficiency was a constant value equal to 1 m^3/MPa when the reservoir pressure was equal to the transition pressure. Moreover, the desorption efficiency was 2.59 m^3/MPa at the sensible pressure and 0.55 m^3/MPa at the threshold pressure.

2.4.5. Surface free energy

Theoretically, under a certain temperature T and pressure P, the free energy of a solid surface at equilibrium is:

Table 3
Desorption characteristic pressures.

Characteristic pressure	Equation	Desorption efficiency (m^3/MPa)
Threshold pressure	$((7+\sqrt{41})/4)^{1/4}\alpha - P_L$	0.55
Transition pressure	$\alpha - P_L$	1
Sensible pressure	$((7-\sqrt{41})/4)^{1/4}\alpha - P_L$	2.59

$$d\sigma = -RT\Gamma d\ln P = -d\pi \tag{10}$$

where σ is the surface free energy in J mol^{-1}; π is the surface pressure in Pa; Γ is the surface excess in mol m^{-2}; R is the universal gas constant equal to 8.314 J mol^{-1} K^{-1}; T is the equilibrium temperature in K; and P is the equilibrium pressure in Pa.

By integrating Eq. (10), the surface pressure could be expressed as follows:

$$\pi = -\int d\sigma = \sigma_0 - \sigma = \int_0^P RT\Gamma d\ln P \tag{11}$$

where σ_0 was the surface free energy under vacuum and σ was the surface free energy after that the coal adsorbed the methane. From Eq. (11), it could be concluded that the surface pressure was equal to the reduced value of the surface free energy because it was compared with the surface free energy under vacuum, π could be called surface free energy.

The formula of the surface excess was:

$$\Gamma = \frac{n}{S} = \frac{V}{V_{std}S} \tag{12}$$

where n was the adsorbed methane volume by unit of mass absorbent in cm^3; V was the adsorbed volume under a pressure Pin cm^3 g^{-1}; V_{std} was the molar volume of a methane equal to 22.4×10^3 cm^3 mol^{-1}; and S was the specific surface area in m^2 g^{-1}.

The Langmuir adsorption isotherms were used to calculate the adsorbed volume V (Pan and Connell, 2007) and π was calculated by substituting Eq. (12) in Eq. (11).

$$\pi = \int_0^P RT\Gamma d\ln P = \int_0^P RT\frac{V}{V_{std}S}d\ln P = \frac{RT}{V_{std}S}\int_0^P \frac{ab}{1+bP}dP$$
$$= \frac{aRT}{V_{std}S}\ln(1+bP) \tag{13}$$

According to the specific surface-area data measured by a low-temperature nitrogen adsorption method and the Langmuir isotherms fitting the characteristic parameters a and b could be determined. The parameter a was the maximum adsorption volume measured under dryness and the parameter b was the inverse of P_L. The variations of the characteristics of the coal surface free energy depending on the pressure were calculated for the different fluids.

3. Results

3.1. Adsorption isotherms

The adsorption isotherms of the raw coal and treated coal samples exhibited shapes of type I isotherm (Fig. 2), according to the IUPAC classification (Sing et al., 1985). This type of isotherm is common for microporous solids and is also named the Langmuir isotherm (monolayer coverage). The adsorption curves increased rapidly and were very similar with minimal differences in the adsorption volume at low pressure. At high pressures, when the surface adsorption was expected to occur, the adsorption curves were flat and differentiated from each other. The adsorption volume decreased in the following order: raw coal, formation water, clean fracturing fluid, active water fracturing fluid, and guar gum fracturing fluid.

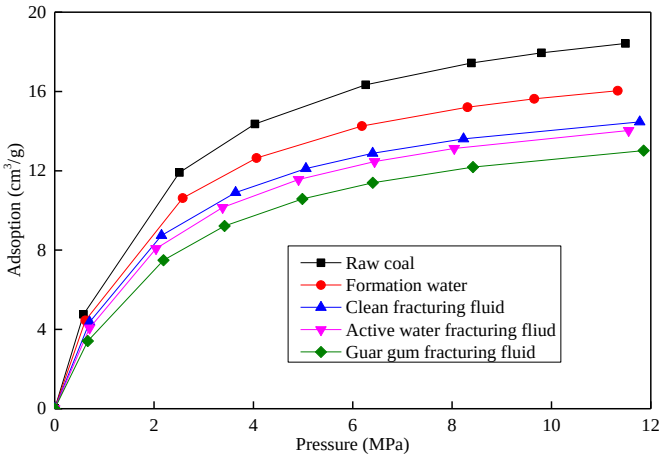

Fig. 2. Adsorption isotherm when the samples were treated by different fracturing fluid.

The adsorption parameters of the coal samples were obtained by using the Langmuir and Freundlich models (Table 4). The Langmuir volume represents the maximum monolayer adsorption of methane and the Langmuir pressure is the inverse indicator representing the affinity of the methane to the coal (Zhang et al., 2014; Gensterblum et al., 2013). The Langmuir volume of the immersed coal samples by formation water and fracturing fluid declined comparatively with the raw coal sample. The Langmuir pressure of the immersed coal had a native relation with the Langmuir volume, indicating that the adsorption capacity of coal was reduced after a fracturing fluid immersion. The influence of the clean fracturing fluid on the adsorption was weakest when compared to all the samples. The adsorption parameters n and k obtained by the Freundlich model decreased after a fracturing fluid immersing, supporting the decreased in adsorption capacity by the fracturing fluid.

3.2. Desorption characteristics

The desorption isotherms of the raw coal and treated coal by

Table 4
Adsorption parameters obtained by the Langmuir and Freundlich models.

Fluid	V_L (cm^3/g)	P_L (MPa)	n	k
Raw coal	21.74	2.07	2.23	6.77
Formation water	18.87	2.00	2.26	6.05
Guar gum fracturing fluid	15.63	2.38	2.17	4.71
Active water fracturing fluid	16.67	2.17	2.18	5.23
Clean fracturing fluid	16.95	2.02	2.16	5.50

fracturing fluids varied (Fig. 3), indicating that the desorption characteristics were much more complicated than expected. These results were describing a typical situation of adsorption hysteresis, where the Langmuir parameters of the methane desorption were smaller than those for the adsorption of both the raw and treated samples (Wang et al., 2014). In the initial stage of desorption, the shape of the curves was relatively flat, meaning that a little amount of methane was desorbed from the coal during this stage. The initial pressure drop minimally contributed to the increase of the desorption volume while the desorption curves declined when the pressure decreased, thus the desorption volume for one unit of pressure obviously increased. Furthermore, desorption hysteresis was also observed for the isotherms of the raw and immersed coal samples.

In order to determine the desorption characteristics of the raw and immersed coal, the characteristic pressures were calculated by applying the defined equations and the results are listed in Table 3. The characteristic pressure of immersed coal by fracturing fluid was reduced compared with the raw and immersed coal treated with formation water. Therefore, a greater pressure drop was required to trigger an effective desorption. The progress of desorption could be divided into four stages: the non-efficient desorption, slow desorption, rapid desorption, and sensible desorption when the threshold pressure, transition pressure, and sensible pressure were taken as the cutting points (Table 5). The stages of rapid and sensible desorptions determined the potential production of the CBM wells. The desorption areas of the immersed coal samples were changing at low pressures as observed by the difference between the three characteristic pressures. The effective desorption area narrowed with the decrease of the area during the rapid and sensible desorptions.

3.3. Variations of the surface free energies

The variations of the surface free energy depending on the increase of pressure at constant temperature are shown in Fig. 4. The

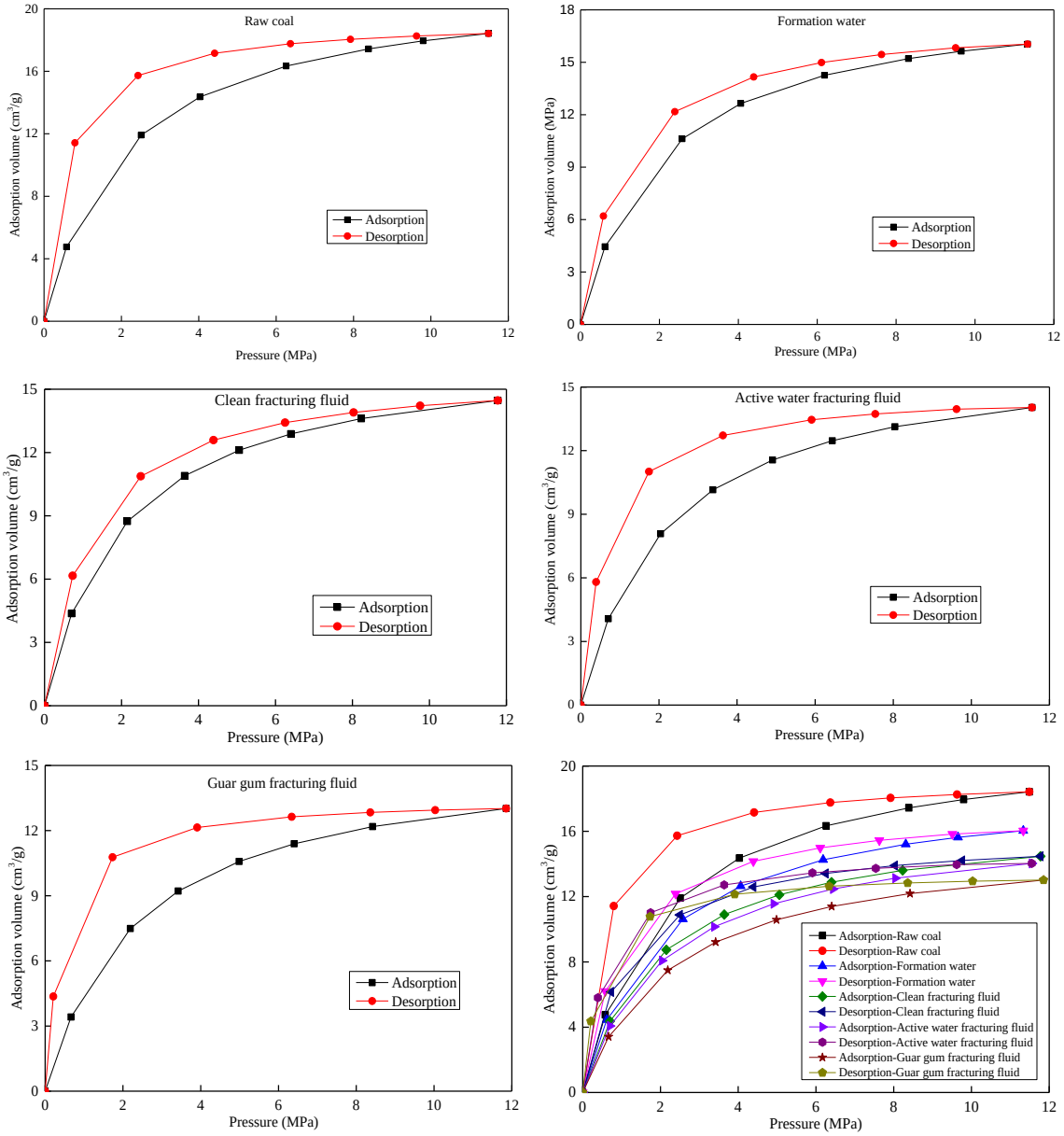

Fig. 3. Adsorption and desorption isotherms of the samples treated with different fracturing fluids.

Table 5
Desorption characteristic pressures of immersed coal.

Fluids	Sensible pressure (MPa)	Transition pressure (MPa)	Threshold pressure (MPa)
Raw coal	2.10	4.64	7.00
Formation water	1.82	4.14	6.31
Guar gum fracturing fluid	1.41	3.72	5.87
Active water fracturing fluid	1.57	3.84	5.96
Clean fracturing fluid	1.62	3.83	5.89

surface free energy increased together with the pressure, similar to the trend observed for adsorption. There was a positive correlation between the change of the surface free energy and the one of methane adsorption. The value of surface free energy was different between the raw and the immersed coal samples. The surface free energy decreased in the following order: formation water, clean fracturing fluid, active water fracturing fluid, and guar gum fracturing fluid. The variation the surface free energy was more important during desorption than during adsorption. Therefore, coal had a stronger adsorption ability to methane during desorption, causing the desorption hysteresis and exhibited a higher adsorption volume during desorption than during adsorption. This theoretical analysis was consistent with the experimental results.

4. Discussion

4.1. Changes in the pore structure

Relatively flat surfaces were selected for the observation of the microstructure of the coal samples before and after fracturing fluid immersion by SEM. The SEM images before and after fracturing fluid immersion were enlarged 1000–5000 times for the study of pores fractures. The raw coal sample exhibited numerous mesopores and macropores, which provided space for methane storage (Fig. 5a, b). The fractures were widely developed in the raw coal sample and provided an effective fluid seepage channel (Fig. 5c). The structural characteristics of the pores and fractures provided space for methane storage, and affected the behavior of methane transport. After the fracturing fluid immersion, many pores were filled with foreign material and some were even blocked (Fig. 5d, e). The fractures also retained solid from the fracturing fluid (Fig. 5e, f). Thus, the channels for methane transport were hindered after the fracturing fluid immersion. As a consequence, the pressure was influenced by the decrease of permeability. Furthermore, the effective desorption of methane was hindered after the fracturing fluid immersion.

4.2. Changes of the surface functional groups

The transformation of the functional groups on the coal surface were monitored by FTIR (Budinova et al., 1998; Wang et al., 2004). The impact of the fracturing fluid on the coal surface functional groups was investigated by comparing the samples treated with different fracturing fluids with the immersed coal by formation water. In order to enhance the change of wave number after the different fluid immersions, different baselines were selected for each fluid. The infrared spectra are shown in Fig. 6. The coal sample immersed in the guar gum fracturing fluid presented sharp absorption peaks between 3700 and 3500 cm^{-1}. The intra- or intermolecular hydrogen bonds at the surface were broken and more –OH functional groups were generated. The bands in the region of 1900–1300 cm^{-1} broadened and the peak at 1740 cm^{-1} disappeared. The results indicated that the free carboxylic acid groups reacted among themselves, shifting the characteristic bands to lower wave numbers. The bands of the coal sample immersed by active water fracturing fluid broadened between 1900 and 1300 cm^{-1} but the intensity of the small peak enhanced, indicating that the conjugated effect of the chemical groups was remarkable and that the ratio of the free carboxylic acid increased. The band of the coal sample immersed in the clean fracturing fluid shifted significantly to higher wave numbers in the characteristic –OH region. We observed many small sharp peaks with free features. A broad absorption peak appeared at 3500 cm^{-1} and was actually the superposition of multiple –OH stretching vibration bands. The absorption peak of the –OH stretching vibration shifted to a lower wave number due to the reinforcement of hydrogen bonding. The broad peak featuring the conjugated multiple groups appeared in the range of 1900–1300 cm^{-1}. The peaks displayed in the typical area of the –COOH chemical group shifted to lower wave numbers, reflecting the conversion from the free to the associated states.

In conclusion, the magnitude and type of inter- and intramolecular hydrogen bindings of the coal sample changed after the fracturing fluid immersion, mostly for the characteristic bands of

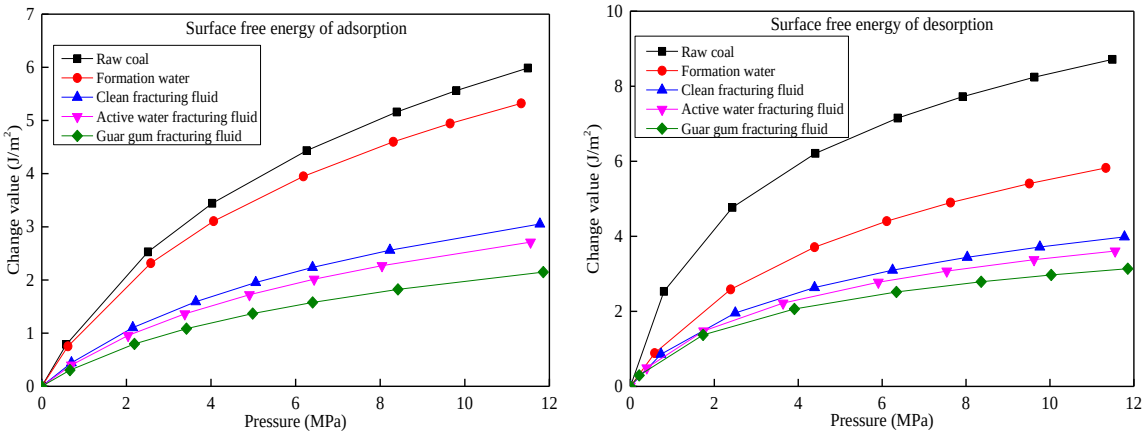

Fig. 4. Surface free energy of adsorption and desorption.

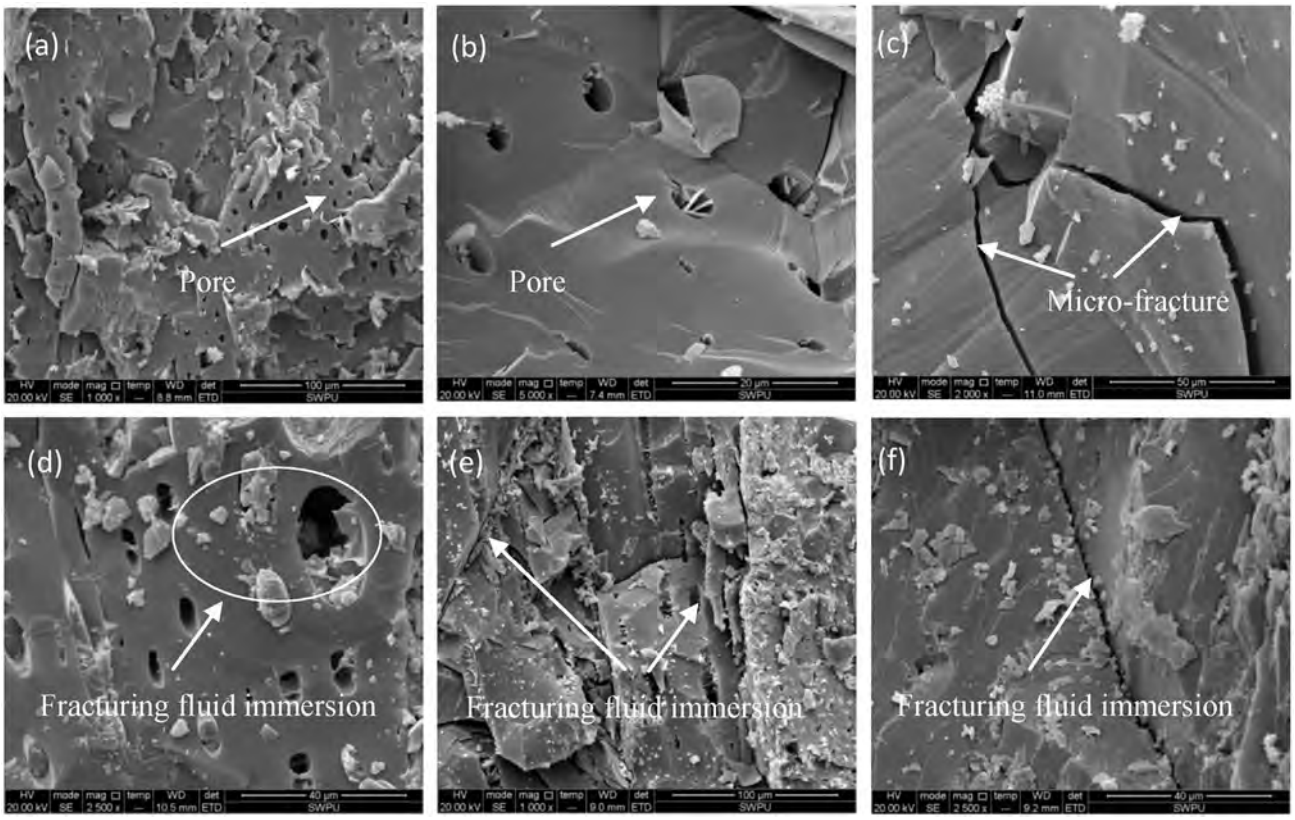

Fig. 5. Micrographs of coal samples before and after fracturing fluid immersion.

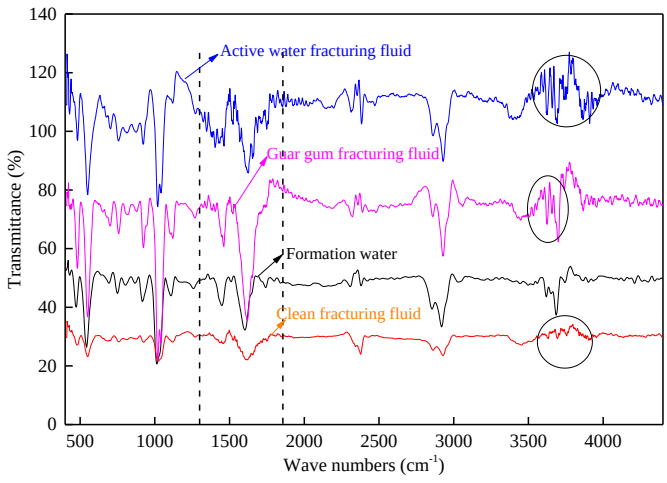

Fig. 6. FTIR spectra of the coal samples immersed in different fracturing fluids.

−OH and −COOH chemical groups, prompting the conversion between the free and the association states. The surface properties of the coal were thus changed after immersion. The guar gum fracturing fluid showed a minimal impact on the surface functional groups of the coal sample. Nevertheless, the active water fracturing fluid and the clean fracturing fluid had a greater influence on the surface functional groups of the coal samples.

4.3. Changes in the solid-liquid interactions

In general, the oxygen-containing functional groups belong to the primary hydrophilic groups of coal (Hao et al., 2013; Zhang et al., 2015; Xia and Yang, 2014). In order to investigate the characteristics of the solid-liquid interactions, the wetting contact angles and the spontaneous imbibition of the samples treated with the formation water and the fracturing fluids were conducted. The wetting contact angle was used to evaluate the wettability between the liquid and solid surfaces. A smaller wetting contact angle indicated that the liquid was easier to spread on the solid surface. The results are shown in Table 6. The values of the fracturing fluids samples were higher than that of the formation water treated sample, indicating that the fracturing fluids had a higher wetting capacity than the formation water.

The imbibition experiments were conducted for coal samples treated with the formation water and the fracturing fluids. The parameters of the coal sample are shown in Table 7. In order to model the in situ experimental conditions, the coal samples were initially saturated with water. The Fig. 7 shows the imbibition characteristics of the coal samples treated with the formation water and the fracturing fluids. The results corroborate the ones from the wetting contact angle measurements. When the contact angle

Table 6
Results of coal wetting angle measurements.

Fracturing fluid	Value (°)	Measurement picture
Formation water	71.69	
Guar gum fracturing fluid	48.18	
Active water fracturing fluid	54.29	
Clean fracturing fluid	58.96	

Table 7
Parameters of the imbibition of coal samples.

Fracturing fluid	Porosity (%)	Permeability (10^{-3} μm^2)	Pore volume (cm^3)	Dry weight (g)	Initial water saturation (%)
Formation water	4.88	0.704	0.929	32.230	19.34
Active water fracturing fluid	4.88	0.428	1.567	26.852	14.56
Clean fracturing fluid	4.39	0.369	1.267	28.328	18.76
Guar gum fracturing fluid	3.91	0.553	1.538	26.722	17.65

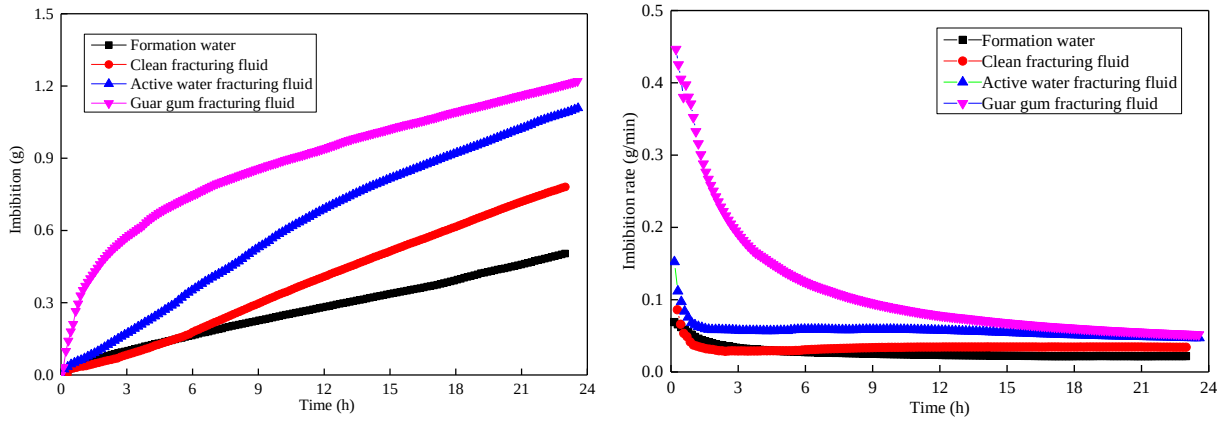

Fig. 7. Evolution of the imbibition value of the coal samples treated with the different fracturing fluids.

decreased, a net decrease in the liquid imbibition quantity appeared. Higher imbibition rates lead to higher imbibition volumes. When more fracturing fluid was applied in the coal matrix, the methane desorption decreased.

5. Conclusions

In this work, we studied experimentally methane adsorption and desorption before and after the fracturing fluid immersion. The purpose was to investigate the effect of the type of fracturing fluid on methane adsorption and desorption. The pore structures and surface properties were also analyzed using infrared spectroscopy, SEM, and wetting contact angle and imbibition methods. The mechanisms controlling the performance of the adsorption and desorption were revealed after the fracturing fluid immersion. On the basis of our work, the following conclusions were drawn:

(1) The presence of a liquid phase reduced the methane adsorption capacity of the coal samples. The Langmuir volume and Freundlich fitting parameters of the coal sample decreased after the fracturing fluid immersion. The surface free energies and adsorbing capacities also reduced, especially for the guar gum fracturing fluid.
(2) The adsorption hysteresis occurred and was influenced by the type of the fracturing fluid. At low pressure, the coal samples were more sensitive to the external fluid immersing, leading to the reduction of desorption efficiency. The characteristic stress of the desorption process reduced, meaning that the coal required a greater pressure drop to enter the effective desorption stage.
(3) The immersion influenced the type and strength of inter- and intramolecular interactions, and impacted on the transformation of the hydroxyl and carboxyl groups of the coal rock, prompting their transformation between the free and associated states.
(4) The SEM results illustrated that the original pores and fractures of the coal rock were seriously hindered after soaking in the completion fluid. Therefore, the permeability reduced, the stress transmission was influenced, and the effective desorption of methane was hindered.
(5) The results of the imbibition experiments corroborated the ones of the wetting contact angle measurements. When the contact angle reduced, a net increase of the quantity of the absorbed liquid occurred. In a word, immersing in a completion fluid for a long time changed the solid-liquid surface properties.

Acknowledgements

The research presented in this paper was financially supported by the United Fund Project of National Natural Science Foundation of China (Grant No.U1262209) and the Nation Basic Research Program of China (973 programs, No. 2013CB228003), Key Fund Project of Sichuan Provincial Department of Education (No. 16ZA0077). These supports are gratefully acknowledged.

References

Beamish, B.B., Crosdale, P.J., 1995. In: Proceedings of the International Symposium Cum Workshop on Management and Control of High Gas Emission and Outbursts. Wollongong, 20-24 March, pp. 353–361.
Budinova, T., Petrov, N., Minkova, V., Razvigorova, M., 1998. Influence of thermo oxidative treatment on the surface properties of anthracite. Fuel 77 (6), 577–580.
Busch, A., Gensterblum, Y., 2011. CBM and CO_2-ECBM related sorption process in coal: a review. Int. J. Coal Geol. 87, 49–71.
Busch, A., Gensterblum, Y., Krooss, B.M., Littke, R., 2004. Methane and carbon dioxide adsorption-diffusion experiments on coal:upscaling and modeling. Int. J. Coal Geol. 60, 151–168.
Chaturvedi, T., Schembre, J.M., Kovscek, A.R., 2009. Spontaneous imbibition and wettability characteristics of Powder River Basin coal. Int. J. Coal Geol. 77, 34–42.
Clarkson, C.R., Bustin, R.M., 1999. The effect of pore structure and gas pressure upon the transport properties of coal: a laboratory and modeling study: 1. Isotherms and pore volume distributions. Fuel 78 (11), 1333–1344.
Chen, S., Zhu, Y., Liu, T., Zhang, C., Yang, H., 2009. Impact of the clear fracturing fluid on the adsorption properties of CBM. J. China Coal Soc. 34 (1), 89–94.
Day, S., Sakurovs, R., Weir, S., 2008. Supercritical gas sorption on moist coals. Int. J. Coal Geol. 74, 203–214.

Gruszkiewicz, M.S., Naney, M.T., Blencoe, J.G., Cole, D.R., Pashin, J.C., Carroll, R.E., 2009. Adsorption kinetics of CO_2, CH_4, and their equimolar mixture on coal from the Black Warrior Basin, West-Central Alabama. Int. J. Coal Geol. 77, 23–33.

Gensterblum, Y., Merkel, A., Busch, A., Krooss, B.M., 2013. High-pressure CH_4 and CO_2 sorption isotherms as a function of coal maturity and the influence of moisture. Int. J. Coal Geol. 118, 45–57.

Ghanbari, E., Dehghanpour, H., 2015. Impact of rock fabric on water imbibition and salt diffusion in gas shales. Int. J. Coal Geol. 138, 55–67.

Hao, S., Wen, J., Yu, X., Chu, W., 2013. Effect of the surface oxygen groups on methane adsorption on coals. Appl. Surf. Sci. 264, 433–442.

Li, X., Kang, Y., Yin, Z., 2014. Surface electricity and wettability of coal rock under the condition of different chemical environments. J. China Univ. Min. Technol. 43 (5), 864–869.

McKee, C.R., Bumb, A.C., Koenig, R.A., 1989. Stress-dependent permeability and porosity of coal and other geologic formations. SPE Form. Eval. 3 (1), 16–19.

Mazzotti, M., Pini, R., Storti, G., 2009. Enhanced coalbed methane recovery. J. Supercrit. Fluids 47 (3), 619–627.

Meng, Y.J., Tang, D.Z., Xu, H., Qu, Y.J., Li, Y., Zhang, W.Z., 2014. Division of coalbed methane desorption stages and its significance. Pet. Explor. Dev. 41 (5), 612–617.

Olsen, T.N., Brenize, G., Frenzel, T., 2003. Improvement processes for coalbed natural gas completion and stimulation. In: Paper SPE 84122 Presented at the SPE Annual Technical Conference and Exhibition, Denver, Colorado, 5–8 October.

Puri, R., King, G.E., Palmer, I.D., 1991. Damage to coal permeability during hydraulic fracturing. In: Paper SPE 21813 Presented at the Low Permeability Reservoirs Symposium, Denver, Colorado, 15–17 April.

Pan, Z.J., Connell, L.D., 2007. A theoretical model for gas adsorption-induced coal swelling. Int. J. Coal Geol. 69 (4), 243–252.

Reeves, S., Pekot, L., 2001. Advanced reservoir modeling in desorption-controlled reservoirs. In: Paper SPE71090 Presented at the SPE Rocky Mountain Petroleum Technology Conference Exhibition in Keystone, Colorado, 21–23 May.

Smith, D.M., Williams, F.L., 1987. Coal Science and Chemistry. Elsevier., Amsterdam, pp. 381–403.

Siemons, N., Wolf, K.–H.A.A., Bruining, H., 2007. Interpretation of carbon dioxide diffusion behavior in coals. Int. J. Coal Geol. 72, 315–324.

Sing, K.S.W., Evereet, D.H., Haul, R.A.W., Pierotti, R.A., Rouquerol, J., Siemieniewska, T., 1985. Reporting physisorpton data for Gas/solid systems with special reference to the determination of surface area and porosity. Pure Appl. Chem. 57 (4), 603–619.

Wang, B.J., Li, M., Zhao, Q.Y., Qin, Y.H., Xie, K.C., 2004. Relationship between surface potential and functional groups of coals. J. Chem. Industry Eng. (China) 55 (8), 1329–1334.

Wang, K., Wang, G., Ren, T., Cheng, Y., 2014. Methane and CO_2 sorption hysteresis on coal: a critical review. Int. J. Coal Geol. 132, 60–80.

Wolf, K.–H.A.A., Barzandji, O.H., Bruining, H., et al., 2003. CO_2 injection for enhanced CH_4 production from coal seams: laboratory experiment and simulations. Proc. Petrotech, New Delhi 9 (12), 329.

Xia, W., Yang, J., 2014. Changes in surface properties of anthracite coal before and after inside/outside weathering process. Appl. Surf. Sci. 313, 320–324.

Zhang, J., Clennell, M.B., Dewhurst, D.N., Liu, K., 2014. Combined Monte Carlo and molecular dynamics simulation of methane adsorption on dry and moist coal. Fuel 12, 186–197.

Zhang, Y., Jing, X., Jing, K., Chang, L., Bao, W., 2015. Study on the pore structure and oxygen-containing functional groups devoting to the hydrophilic force of dewatered lignite. Appl. Surf. Sci. 324, 90–98.